

Emergence of novel magnetic order at finite temperature in overdoped pnictides

Carla Lupo,¹ Thomas Julian Roberts,¹ and Cedric Weber¹

¹*King's College London, Theory and Simulation of Condensed Matter, The Strand, WC2R 2LS London, UK*

We examine the temperature dependence of the magnetic ordering in the frustrated Heisenberg $J_1 - J_2$ model in presence of two different kind of dopants: vacancies or magnetic impurities. We demonstrate that, irrespective to their magnetic ratio, the introduction of impurities quenches the order by disorder selection mechanism associated with an Ising-like phase transition at low temperatures and gives way to a 90° (antiferromagnetic) order. The presence of dopants triggers a non trivial competition between entropically selected states (collinear) and energetically favoured ones (antiferromagnetic) in dependence of both dilution and temperature. While in case of magnetic impurity, the interesting magnetic phases are observed for full range of temperature and doping, in case of nonmagnetic impurities every magnetic order is destroyed at all temperatures above 12% dilution. At fixed low temperature and tuning the doping we show a first order phase transition leading to the re-entrance of the Ising-like order with percolation of islands of 90° order. At fixed doping and varying the temperature we observe a transition from the antiferromagnetic to the collinear phase assisted by a new emerging magnetic phase in the presence of magnetic impurities, whilst in case of vacancies this transition is characterised by a coexistent region of both. Furthermore, tuning the magnetic moment of the impurities, a complete collapse of the Ising-like order is attained. This is in agreement with observations of Ir dopant atoms in superconducting $\text{Ba}(\text{Fe}_{1-x}\text{Ir}_x)_2\text{As}_2$ with $x < 0.047$.

Unconventional superconductivity occurs in the proximity of magnetically ordered states in many materials [1, 2]. Understanding the magnetic phase of the parent compound is an important step towards understanding the mechanism of superconductivity. While for cuprates magnetism and the underlying electronic state is understood there is still debate in the case of iron pnictides BaFe_2As_2 [3]. Many low-energy probes such as resistivity [4], scanning tunnelling microscopy [5] and angle-resolved photoemission spectroscopy [6] have measured strong in-plane anisotropy of the electronic states, but there is no consensus on its physical origin. It was suggested from first principle calculations [7] that the origin stems from orbital order, but the obtained anisotropy in the resistivity is opposite to the one found experimentally [8]. A more likely scenario supported by recent neutron diffraction measurements [9] is related to a spin density wave instability due to the presence of electron and hole pockets around $\mathbf{k} = (\pi, 0)$ and $\mathbf{k} = (0, \pi)$. The resulting magnetic order is of nematic type and can be seen as a helicoidal magnetic state with pitch vector $\mathbf{Q} = (0, \pi)$ or $\mathbf{Q} = (\pi, 0)$. Since the orbital character of the electron and hole pockets depends on the wave vector of the instability[10], the nematic order introduces in turn an orbital polarization. To describe the low-energy magnetic properties of this system, it has been suggested early on that a local moment picture may become relevant in the presence of moderately large electronic correlations[11], leading to the Heisenberg model with both nearest- (J_1) and next-nearest (J_2) exchange couplings defined by

$$\hat{H} = J_1 \sum_{\langle i,j \rangle} \hat{\mathbf{S}}_i \cdot \hat{\mathbf{S}}_j + J_2 \sum_{\langle\langle i,j \rangle\rangle} \hat{\mathbf{S}}_i \cdot \hat{\mathbf{S}}_j, \quad (1)$$

in the collinear regime, both J_1 and J_2 are positive, and $2J_2 > J_1$ [12]. In this expression, $\hat{\mathbf{S}}_i$ are $O(3)$ spins on a

periodic square lattice with $N = L \times L$ sites. $\langle i, j \rangle$ and $\langle\langle i, j \rangle\rangle$ indicate the sum over nearest and next-nearest neighbors, respectively [32].

The first attempt at fitting the experimental spin density wave excitation spectra with a Heisenberg model suggested that one should use very anisotropic values of J_1 [13]. However, it was later shown that the fits of the experimental data included energy scales beyond 100 meV, which are not well described by magnon excitations [14]. A more careful study, including the itinerant character of the electrons[15], led to the conclusion that pnictides are indeed in the collinear regime with $(\mathbf{Q} = (0, \pi), (\pi, 0))$ magnetic instabilities, a conclusion supported by first-principle calculations for selenium based compounds (KFe_2Se_2) [16]. We also note that it was also recently argued[17] that to get a proper description of magnetic interactions and spin fluctuations in ferropnictides, additional biquadratic interactions might be important.

In parallel, it has been suggested both experimentally [18, 19] and theoretically [20] that impurities have a dramatic impact on the magnetic and superconducting properties. In particular, recent magnetic polarized x-ray measurements suggest that a new type of magnetic order emerges due to the presence of magnetic impurities in BaFe_2As_2 [21]. Furthermore, periodic ordering of supercell structures of vacancies in $\text{TlFe}_{1.6}\text{Se}_2$, observed by electron microscopy, were shown to induce a spin reorientation in these structures [22, 23]. All these results, together with results obtained a few years ago on a layered vanadium oxide [24], call for an in-depth investigation of the effect of impurities in this frustrated Heisenberg model.

In this letter we build upon our earlier calculations in Ref[25] by extending the calculations to samples doped

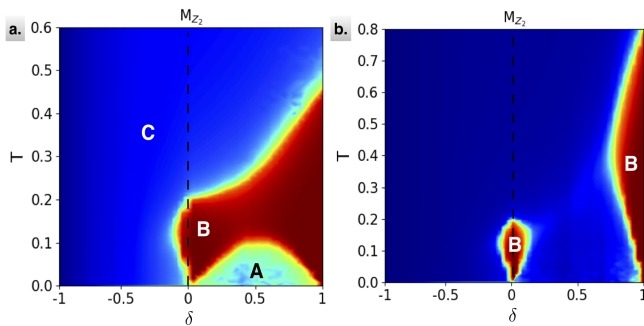


Figure 1: (color online) Color maps of the Ising (M_2) order in function of temperature and dilution for a $L \times L = 50 \times 50$ lattice. Negative and positive dilution refers respectively to doping with non magnetic impurities and with magnetic ones $r = 1.5$ (a) and $r = 2$ (b). Colours range from blue (minimum) to red(maximum). From low to high temperature different ordered region can be distinguished: A) anticollinear, B) collinear and C) weak Néel state.

with both magnetic and non-magnetic impurities, exploring highly doped lattices (up to full doping). In particular, we focus on the competing magnetic order at high doping, which corresponds to optimally and overdoped pnictide samples. We address the question of the interplay between the frustration induced by the exchange couplings and the disorder induced by the imperfections of the crystallographic structure. Increasing the doping we expect the possibility of first order phase transitions driven by a percolation mechanism, where impurities drive local fluctuating order parameters on short distances and become long range at high dilutions.

Since density functional calculations, and quite generally quantum based calculations, are limited to relatively small unit-cells and cannot tackle the issue of large super-cell structures we limit our calculations to a frustrated classical model [26], and carry out Monte Carlo calculations of the Heisenberg $J_1 - J_2$ model in the presence of impurities using the same numerical approach as in Refs. 27, 28. We limit ourselves to 50×50 lattice sizes (2500 correlated atoms), but average over large numbers of disordered configurations (up to 5000 configurations) by using a BlueGene/Q supercomputer facility. In the absence of disorder and at zero temperature, the magnetic vector is $\mathbf{Q} = (\pi, \pi)$ for $J_2/J_1 < 0.5$, and for $J_2/J_1 > 0.5$ the ground state is continuously degenerate and is characterised by a bi-partite lattice, with two distinct anti-ferromagnetically ordered states on each sub-lattice, with θ the angle between the two magnetic directions. At finite temperature the entropy selection reduces the $O(3)$ symmetry of the ground state to Z_2 selecting the states with antiferromagnetic spin correlations in one spatial direction and ferromagnetic correlations in the other ($\mathbf{Q} = (0, \pi), (\pi, 0)$). This is the so-called *order*

by disorder entropic selection and the associated discrete symmetry breaking drives a finite temperature Ising-like phase transition [27, 29]. We address how the presence of disorder affects this transition.

We first examine the phase diagram of both doping regimes where the magnetic moment of the doping (r) is characterized by its ratio to the magnetic moment of the undoped compound (M_{Fe} for iron), $r = M_{imp}/M_{Fe}$. The dilution is denoted as $\delta > 0$, $\delta < 0$ for $r \neq 0$ and $r = 0$ respectively. In Fig. 1 we consider the collinear order parameter constructed from the original spin variables $\hat{\mathbf{S}}_i$

$$M_2(x) = (\hat{\mathbf{S}}_i - \hat{\mathbf{S}}_k) \cdot (\hat{\mathbf{S}}_j - \hat{\mathbf{S}}_l), \quad (2)$$

where (i, j, k, l) are the corners with diagonal (i, k) and (j, l) of the plaquette centered at the site x of the dual lattice [see Fig. S1(a)], and we define its normalized counterpart as $Z_2(x) = M_2(x)/|M_2(x)|$. In this way, the two collinear states with $\mathbf{Q} = (\pi, 0)$ and $\mathbf{Q} = (0, \pi)$ can be distinguished by the value of the Ising variable, $Z_2(x) = \pm 1$. For impurities with a 50% larger magnetic moment (see Fig. 1(a), $\delta > 0$), we observe that there exists a temperature range $T = (0.1, 0.2)J_1$ where the collinear order survives at all dilutions. However, the transition from collinear to paramagnetic (from region B to C) at high temperature increases from 0.2 to 0.45. This can be explained by a very simple argument; in the fully doped regime all spins are 1.5 times larger and so the energy scales are rescaled by a factor 1.5^2 , increasing T_c in turn by a factor 2.25. Differently from the case with $r = 1.5$, we observe that the Ising-like order is rapidly suppressed by doping with non-magnetic $r = 0$ impurities (Fig. 1(a), $\delta < 0$) or impurities with a large magnetic moment $r = 2$ (Fig. 1(b), $\delta > 0$), with no collinear magnetic order obtained beyond 8% dilution. This is expected for the case of non-magnetic dopants, where large dilutions prevents the propagation of long-

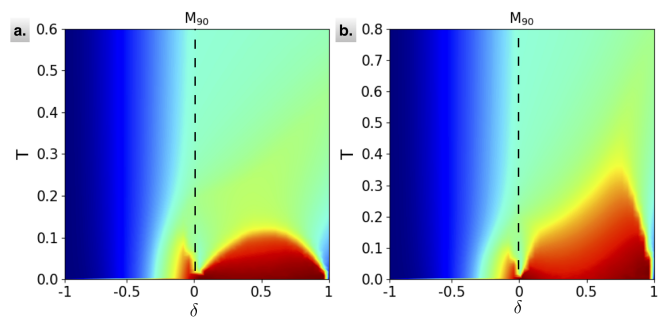


Figure 2: (color online) Color maps of the 90 degree (M_{90}) order in function of temperature and dilution for a $L \times L = 50 \times 50$ lattice. Negative and positive dilution refers respectively to doping with non magnetic impurities and with magnetic ones $r = 1.5$ (left panel) and $r = 2$ (right panel). Colours range from blue (minimum) to red(maximum).

range magnetic order as the magnetic order propagates by short-range correlations. The quenching of low energy fluctuations upon the introduction of non-magnetic impurities have been observed experimentally both in vanadates [30] and pnictides [19]. Although the Ising order survives for $\delta > 0$, if we look at fixed dilution, $\delta = 50\%$, we observe that the collinear order is also suppressed at low temperature (region A), and we obtain a re-entrance transition of the collinear order (region A to B). This is expected at low temperature and low doping; it has been shown that around a single impurity the degeneracy of the ground-state of the $J_1 - J_2$ model is lifted and the 90° magnetic order is selected from the manifold by an energy optimization process [1, 31]. Note that this latter mechanism is driven by an energy optimization and is not expected to survive to high temperatures. In Fig. 2a,b we report the antiferromagnetic order

$$M_{90}(x) = |(\hat{S}_i - \hat{S}_k) \times (\hat{S}_j - \hat{S}_l)| \quad (3)$$

where (i, j, k, l) defines the same plaquette as in Eq.2 [see Fig. S1(a)].

Our results confirm that the order stabilized in region A in Fig. 1a is the 90° order. Local fluctuations of the 90° order around impurities percolate and form a stable order at low temperature. At high temperature the entropic contribution dominates and the Ising-like order is recovered (Fig 1.a, $\delta > 0$). Note, however, that if the magnetic moment of the dopant is large ($r = 2$), the entropic contributions aren't able to recover the collinear order and the 90° order surprisingly stabilizes at high temperature until the paramagnetic phase is obtained (Fig. 2b, $\delta > 0$ and Fig. 1.b $\delta > 0$), leading to a suppression of the Ising order in between the undoped and fully doped regions. This has been observed in the superconducting pnictides doped with Ir [21] where the collinear order is suppressed when the dilution is greater than $\delta > 0.047$. This is in agreement with the quenching of the collinear phase observed as impurity ratio $r = 2$ in the doping region $\delta = [0.2, 0.8]$. Indeed in Fig. 2b we can clearly see that at approximately half doping the low temperature range is fully dominated by the antiferromagnetic order M_{90} being the collinear order, M_{Z_2} equal to zero Fig. 1b. Note that this mechanism is not obtained by doping with non-magnetic impurities (Fig. 1a $\delta < 0$ and Fig. 2a $\delta < 0$), as the suppression of the Ising-like order is not concomitant with the stabilization of a competing order.

In the dilution range $\delta < 0.2$ and $\delta > 0.8$, the competition between the entropic and the energetic contribution is restored and interestingly we observed that the re-entrance transition (region A to B, Fig 1b, 2a) is characterized by a sharp cross over. This mechanism is rationalized in Fig. 3a, where we considered a single impurity case. We observe that the cross-over is characterized by a magnetic phase (Fig 3c) different from both the antiferromagnetic (Fig 3b) and the collinear case (Fig 3c). This

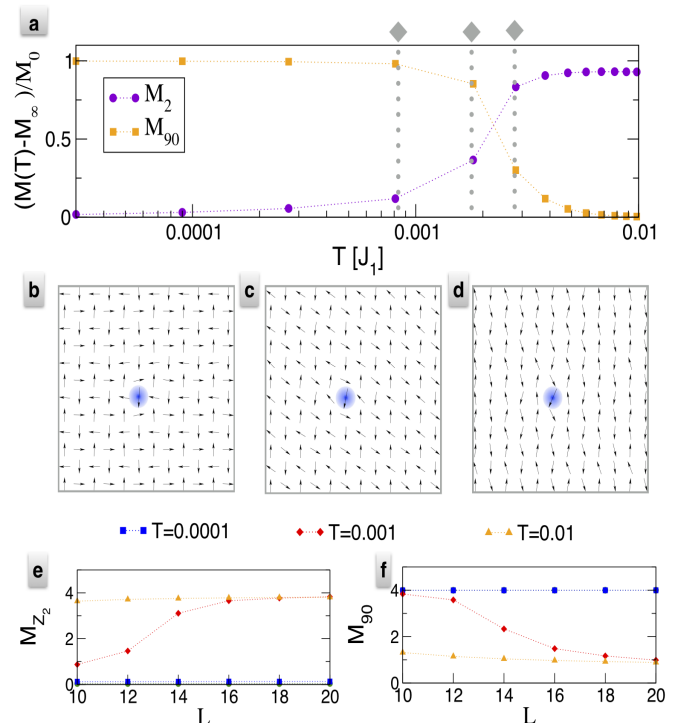


Figure 3: Single magnetic impurity case with $r = 1.5$. a) Temperature dependence of M_2 and M_{90} for a lattice with $L = 12$. b)-c)-d) Typical spin configuration obtained at three fixed temperatures at $T = 0.0008, 0.00181, 0.00281 J_1$. e)- f) respectively collinear and antiferromagnetic order parameter values for fixed temperatures $T = 0.0001, 0.001, 0.01 J_1$ in function of different lattices with linear dimension L .

intermediate phase consists of two distinct antiferromagnetically ordered states on two sublattices with a relative angle α between their magnetization axis which is selected by the impurity spin direction.

This suggests that there is a crossing of the free energies of the 90° and collinear orders at the transition, where the competition in the free energies $F = E - T * S$ happens between the energy term E and entropic contribution $T * S$. As this process is very much dependent on the local disorder configurations, the temperature associated with the sharp cross-over is also dependent on the disorder configurations. In an experiment, or in our computed physical observables which are averaged over large disorder samples, the transition is a smooth cross-over, hiding the physical explanation related to the competition of energetic and entropic terms. Remarkably, the mechanism which determines the *energy vs entropy* competition is different respective to vacancies or magnetic doping. Indeed in case of non magnetic impurity the transition between the antiferromagnetic and the collinear phase is happening through a coexistent phase: it was shown (Ref [25]) at finite temperature the antiferromagnetic order stabilizes locally around the impurity and with the

collinear states recovered outside this region. Instead, in case of magnetic impurities, we observe that the magnetic phase which characterizes the crossover is not a co-existent phase of collinear and anticollinear order. The transition between the 90° and collinear order is rationalized with respect to the lattice size in Figs 3a-b, where we show both the order parameters at three different temperatures, $T = 10^{-4}, 10^{-3}, 10^{-2}J_1$, for a single impurity embedded in a lattice of size $L = (10, 20)$. Note that periodic conditions are used in this simple model, such that the lattice size mimics the average distance between impurities at high dilutions. At low temperature $T = 10^{-4}$, as entropic contributions are absent, we observe that the 90° order dominates as expected for all cases (analytic argument at $T = 0$ in suppl mat. Fig S1b). As temperature is increased to $T = 10^{-3}$ and $T = 10^{-2}$, we observe that the 90° degree is stabilised at small L , but the collinear order wins in larger lattices where the entropic contributions in turn become larger. This illustrates the mechanism obtained around the large dilution (small L), where the 90° order is stabilized, and at low dilutions (large L), where the collinear order wins.

Further insights about the transition between the different magnetic phases is shown in Fig. 4. For doping with magnetic impurities (Fig. 4a-b), we obtain as expected a large peak in the specific heat at the transition associated with the loss of the collinear order (region B to C, Fig. 4a $\delta > 0$). As we do not observe a drop in the specific heat along the Ising-like transition in Fig 4a (where $r = 1.5$), we conclude that the transition remains second order along this line. Surprisingly a continuous second order also in Fig 4b (with $r = 2$) at the transition between the anticollinear and the paramagnetic phase, even if the Ising-like order is zero for all T . In more detail, at fixed dilution $\delta = 25\%$ we observe that the melting of the anticollinear order occurs with a cross over associated with a non divergent peak of the specific heat (Fig. 4d). Note that the specific heat also indicates fluctuations at the re-entrance transition (region A to B). Thus for a critical $r_c < 2$, the intersection of the different magnetic phases turns into three-critical crossing points.

For doping with non-magnetic impurities we observe the irising of the peaks for the Ising-like transition (fixed low doping) which is consistent with what observed so far in case of magnetic impurities. A more interesting and novel behaviour is observed at fixed low temperature where there exists a continuous pathway which does not involve any sharp transition. This is crucial for applications because it does not involve any energy cost. This was not observed in the previous work because no fluctuations were considered. At zero temperature we observe that there are no energy fluctuations associated with the percolation transition which is instead indicated by the sudden disappearance of the susceptibility at 8% in Fig. S5 (suppl mat) typical of a first-order transition.

In conclusion we found that the order by disorder en-

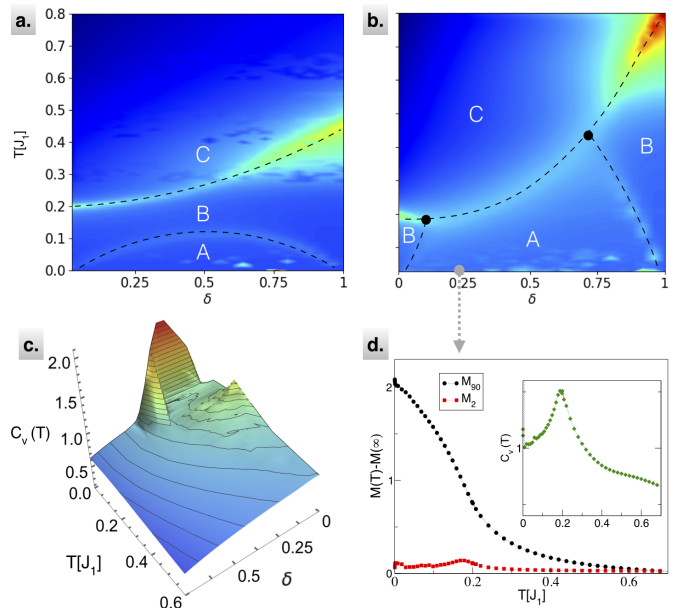


Figure 4: (color online) Color maps of the specific heat in function of temperature and dilution for a $L \times L = 50 \times 50$ lattice respectively for magnetic impurities $r = 1.5$ (a) and $r = 2$ (b). Colours range from blue (minimum) to red (maximum). Black dashed lines are guide to the eyes to distinguish the three ordered states: A (anticollinear), B (collinear) and C (paramagnetic).

trophy selection, associated with the Ising-like phase transition that appears for $J_2/J_1 > 1/2$ in the pure spin model, is quenched at low temperature due to the presence of impurities. Indeed, irrespective of the magnetic ratio of the dopant an anticollinear order is stabilized around the impurities, which in turn induces a reentrance of the Ising-like phase transition. The melting of the collinear order happens in two directions and via two different mechanisms: i) through a percolation transition from increasing dilution (at fixed temperature) and ii) via a sharp cross-over due to the energetic versus entropic contribution increasing temperature (at fixed doping). While the former exists irrespective to the nature of the dopant the latter is highly affected by the ratio of the magnetic impurities.

Acknowledgments C.L. is supported by the EP-SRC Centre for Doctoral Training in Cross-Disciplinary Approaches to Non-Equilibrium Systems (CANES, EP/L015854/1). C.W. gratefully acknowledges the support of NVIDIA Corporation, ARCHER UK National Supercomputing Service. We are grateful to the UK Materials and Molecular Modelling Hub and the Hartree Centre (Bluegene -Q) for computational resources, which is partially funded by EPSRC (EP/P020194/1).

- [1] Y. Takabayashi, A. Y. Ganin, P. Jeglic, D. Arcon, T. Takano, Y. Iwasa, Y. Ohishi, M. Takata, N. Takeshita, K. Prassides, et al., *Science* **323**, 1585 (2009), ISSN 1095-9203 (Electronic); 0036-8075 (Linking).
- [2] T. Park, F. Ronning, H. Q. Yuan, M. B. Salamon, R. Movshovich, J. L. Sarrao, and J. D. Thompson, *Nature* **440**, 65 (2006), ISSN 1476-4687 (Electronic); 0028-0836 (Linking).
- [3] Y. Kamihara, T. Watanabe, M. Hirano, and H. Hosono, *J Am Chem Soc* **130**, 3296 (2008), ISSN 1520-5126 (Electronic); 0002-7863 (Linking).
- [4] J.-H. Chu, J. G. Analytis, K. De Greve, P. L. McMahon, Z. Islam, Y. Yamamoto, and I. R. Fisher, *Science* **329**, 824 (2010), ISSN 1095-9203 (Electronic); 0036-8075 (Linking).
- [5] T.-M. Chuang, M. P. Allan, J. Lee, Y. Xie, N. Ni, S. L. Bud'ko, G. S. Boebinger, P. C. Canfield, and J. C. Davis, *Science* **327**, 181 (2010), ISSN 1095-9203 (Electronic); 0036-8075 (Linking).
- [6] P. Richard, K. Nakayama, T. Sato, M. Neupane, Y.-M. Xu, J. H. Bowen, G. F. Chen, J. L. Luo, N. L. Wang, X. Dai, et al., *Phys. Rev. Lett.* **104**, 137001 (2010), ISSN 1079-7114 (Electronic); 0031-9007 (Linking).
- [7] W. Lv, F. Krüger, and P. Phillips, *Phys. Rev. B* **82**, 045125 (2010), URL <http://link.aps.org/doi/10.1103/PhysRevB.82.045125>.
- [8] B. Valenzuela, E. Bascones, and M. J. Calderón, *Phys. Rev. Lett.* **105**, 207202 (2010), URL <http://link.aps.org/doi/10.1103/PhysRevLett.105.207202>.
- [9] D. K. Pratt, M. G. Kim, A. Kreyssig, Y. B. Lee, G. S. Tucker, A. Thaler, W. Tian, J. L. Zarestky, S. L. Bud'ko, P. C. Canfield, et al., *Phys. Rev. Lett.* **106**, 257001 (2011), URL <http://link.aps.org/doi/10.1103/PhysRevLett.106.257001>.
- [10] R. M. Fernandes, E. Abrahams, and J. Schmalian, *Phys. Rev. Lett.* **107**, 217002 (2011), URL <http://link.aps.org/doi/10.1103/PhysRevLett.107.217002>.
- [11] Q. Si and E. Abrahams, *Phys. Rev. Lett.* **101**, 076401 (2008), URL <http://link.aps.org/doi/10.1103/PhysRevLett.101.076401>.
- [12] P. Chandra and B. Doucot, *Phys. Rev. B* **38**, 9335 (1988), URL <http://link.aps.org/doi/10.1103/PhysRevB.38.9335>.
- [13] J. Zhao, D. T. Adroja, D.-X. Yao, R. Bewley, S. Li, X. F. Wang, G. Wu, X. H. Chen, J. Hu, and P. Dai, *Nat Phys* **5**, 555 (2009), URL <http://dx.doi.org/10.1038/nphys1336>.
- [14] R. A. Ewings, T. G. Perring, J. Gillett, S. D. Das, S. E. Sebastian, A. E. Taylor, T. Guidi, and A. T. Boothroyd, *Phys. Rev. B* **83**, 214519 (2011), URL <http://link.aps.org/doi/10.1103/PhysRevB.83.214519>.
- [15] I. Eremin and A. V. Chubukov, *Phys. Rev. B* **81**, 024511 (2010), URL <http://link.aps.org/doi/10.1103/PhysRevB.81.024511>.
- [16] C. Cao and J. Dai, *Chinese Physics Letter* **28**, 057402 (2011).
- [17] A. L. Wysocki, K. D. Belashchenko, and V. P. Antropov, *Nat Phys* **7**, 485 (2011), URL <http://dx.doi.org/10.1038/nphys1933>.
- [18] S. Mukhopadhyay, S. Oh, A. M. Mounce, M. Lee, W. P. Halperin, N. Ni, S. L. Bud'ko, P. C. Canfield, A. P. Reyes, and P. L. Kuhns, *New Journal of Physics* **11**, 055002 (2009), URL <http://stacks.iop.org/1367-2630/11/i=5/a=055002>.
- [19] P. Bonfà, P. Carretta, S. Sanna, G. Lamura, G. Prando, A. Martinelli, A. Palenzona, M. Tropeano, M. Putti, and R. De Renzi, *Phys. Rev. B* **85**, 054518 (2012), URL <http://link.aps.org/doi/10.1103/PhysRevB.85.054518>.
- [20] C.-C. Chen, R. Applegate, B. Moritz, T. P. Devereaux, and R. R. P. Singh, *New Journal of Physics* **13**, 043025 (2011), URL <http://stacks.iop.org/1367-2630/13/i=4/a=043025>.
- [21] M. P. M. Dean, M. G. Kim, A. Kreyssig, J. W. Kim, X. Liu, P. J. Ryan, A. Thaler, S. L. Bud'ko, W. Strassheim, P. C. Canfield, et al., *Phys. Rev. B* **85**, 140514 (2012), URL <http://link.aps.org/doi/10.1103/PhysRevB.85.140514>.
- [22] A. F. May, M. A. McGuire, H. Cao, I. Sergueev, C. Cantoni, B. C. Chakoumakos, D. S. Parker, and B. C. Sales (2012), arXiv/1207.1318.
- [23] R. Yu, P. Goswami, and Q. Si, *Phys. Rev. B* **84**, 094451 (2011), URL <http://link.aps.org/doi/10.1103/PhysRevB.84.094451>.
- [24] N. Papinutto, P. Carretta, S. Gonthier, and P. Millet, *Phys. Rev. B* **71**, 174425 (2005), URL <http://link.aps.org/doi/10.1103/PhysRevB.71.174425>.
- [25] C. Weber and F. Mila (2012), 1207.0095, URL <http://arxiv.org/abs/1207.0095>.
- [26] G. Franzese, V. Cataudella, S. E. Korshunov, and R. Fazio, *Phys. Rev. B* **62**, R9287 (2000), URL <http://link.aps.org/doi/10.1103/PhysRevB.62.R9287>.
- [27] C. Weber, L. Capriotti, G. Misguich, F. Becca, M. Elhajal, and F. Mila, *Phys. Rev. Lett.* **91**, 177202 (2003).
- [28] C. Weber, F. Becca, and F. Mila, *Phys. Rev. B* **72**, 024449 (2005), URL <http://link.aps.org/doi/10.1103/PhysRevB.72.024449>.
- [29] P. Chandra, P. Coleman, and A. Larkin, *Phys. Rev. Lett.* **64**, 88 (1990).
- [30] R. Melzi, P. Carretta, A. Lascialfari, M. Mambrini, M. Troyer, P. Millet, and F. Mila, *Phys. Rev. Lett.* **85**, 1318 (2000).
- [31] C. Henley, *Journal of Applied Physics* **61**, 3962 (1987), URL <http://www.scopus.com/inward/record.url?eid=2-s2.0-0001605112&partnerID=40&md5=20cae8398abcd8dc3f2e56a49062e2b9>.
- [32] J_1 sets the energy scale, and in our work we use $J_2/J_1 = 0.55$ is used when not specified otherwise, and both $J_1 > 0$ and $J_2 > 0$.

**Supplementary Material for
"Magnetic impurities in the frustrated
Heisenberg model"**

Dependence on the spin impurity ratio

We would like to investigate the energy gain obtained by the distortion of an angle α around a single impurity with magnetic magnitude r . Since we assume that the anticolinear order is stabilized beyond the next nearest neighbours of the impurity - only the first nearest neighbours are tilted as shown in Fig. S1(a)- we have that the local energy is:

$$E(\lambda = J_2/J_1, \alpha, r)/J_1 = 4 \cos(\pi/2 - \alpha) + 8\lambda \cos(\pi - \alpha) + 4\lambda \cos(\pi - 2\alpha) + 8 \cos(\pi/2 + \alpha) - 12\lambda + 4r(-\lambda + \cos(\pi/2 - \alpha)) \quad (1)$$

As discussed in Ref.[25] the energy gain at zero temperature decreases monotonically when J_2/J_1 increases. The value of $\lambda = J_2/J_1$ above which this energy contribution becomes small depends on the magnitude of the magnetic impurity. Starting from the undoped regime $r = 1$ we expect the energy contribution to be zero. This is explained by the fact that the ground state is described by two sublattices, continuously degenerate with respect to one another, and which have a relative angle θ between their magnetization axis this is the case at $T = 0$.

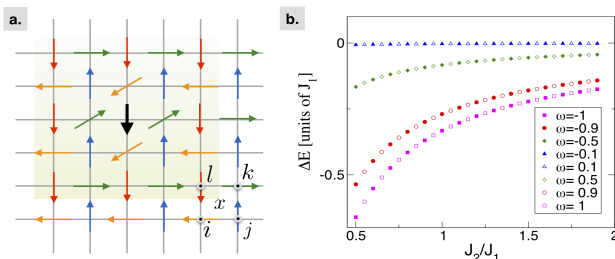


Figure S1: Single impurity case. a) local distortion of the nearest neighbours around the impurity (black arrow) of an angle θ and 90° order outwards. Plaquette representation centered in x with corners (i, j, k, l) on the left bottom side of the picture. b) Energy gain $E(\alpha) - E(\alpha = 0)$ at zero temperature as a function of J_1/J_2 computed with the variational argument in Eq.1 where only the nearest-neighbour sites of the magnetic impurity are distorted by an angle α . Different symbols relate to different spin impurity ratio $r = 1 - \omega$.

We observe that the energetic optimization is symmetric with respect to $\omega = 1 - r$.

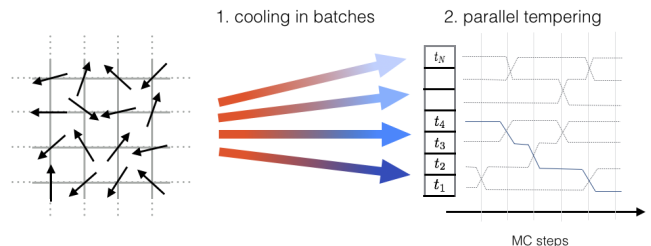


Figure S2: Diagram of the simulation procedure. Starting from a random configuration, we cooled the system in N replicas at adjacent temperatures $\{t_1, \dots, t_N\}$. We then perform parallel tempering starting from these N configurations: an exchange of configuration information is allowed between replicas at adjacent temperatures to prevent the system from being trapped in a local minimum. There is a further parallelization on top of this process which starts from different initial conditions and it is crucial in the final averages evaluation.

Simulation Methodology: heatbath and parallel tempering

Our Monte Carlo simulations were performed by a two-part process with both parts involving the use of a heat bath algorithm Ref.[2] to generate new spin configurations. The first part involved a shorter cooling phase from a high temperature. This process allowed the initially random configurations to slowly approach equilibrium configurations and prevent the system from being trapped in local minima at low temperature.

The second part was the main MC stage where the temperature was kept fixed. In particular to get a better exploration of the phase space we implemented a parallel tempering algorithm.

Parallel tempering (Ref.[3]) involves simulating a number of replicas simultaneously and allowing configurations to be swapped between adjacent temperatures while performing Monte Carlo steps between swaps. This assures that at each step, the configuration at lowest temperature is the one with minimum energy among all the replicas. Replicas are allowed to switch based upon the condition of detailed balance. To enforce this we used the standard Metropolis Monte Carlo condition to decide if swaps between replicas at different temperatures were accepted.

$$\omega_{m \rightarrow n} = \begin{cases} 1 & \text{if } E_m \leq E_n \\ \exp(-(E_n - E_m)/KT) & \text{if } E_m > E_n \end{cases} \quad (2)$$

To achieve the best possible sampling at low temperature we consider batches with temperatures in a geometric progression ($T_i/T_{i-1} = \text{constant}$). Since the computational effort increases on the order of the number of the replicas N , it became crucial the use of large CPU clusters. A further parallelization was used also on top of the schematic representation in Fig. S2 in order to get better

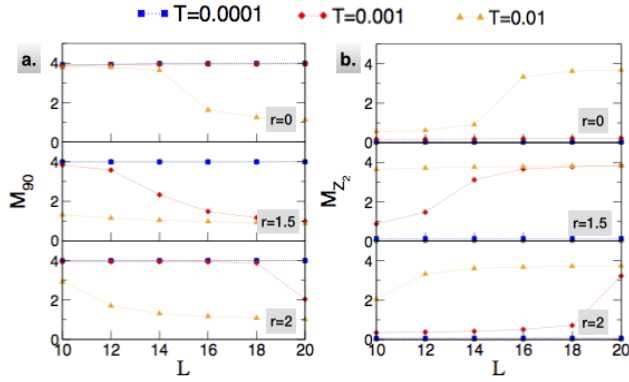


Figure S3: Single impurity case. Anticollinear M_{90} (left) and collinear M_z (right) order obtained by Monte Carlo at fixed $T = 0.00001, 0.0001, 0.001, 0.01J_1$, in case of single magnetic impurity with magnitude $r = 0, 1.5, 2$ in function of different lattices with linear dimension L .

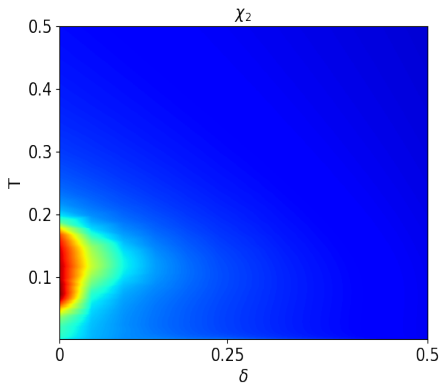


Figure S4: (color online) Color map of the fluctuations χ_{M_z} of the collinear order parameter for the case of doping with vacancies ($r = 0$).

averages of the observables. All our calculations and order parameters were measured during this second stage taking ensemble averages across all spin configurations at a particular temperature. The method originally limited to problems in statistical physics, it was later apply to Monte Carlo simulations of biomolecule. The variety of fields in which it has been generalized include polymers [4], protein [5] and spin glasses [6].

-
- [1] C. L. Henley, Phys. Rev. Lett. **62**, 2056 (1989), URL <http://link.aps.org/doi/10.1103/PhysRevLett.62.2056>.
 - [2] Y. Miyatake, M. Yamamoto, J. J. Kim, M. Toyonaga, and O. Nagai, Journal of Physics C: Solid State Physics **19**, 2539 (1986), URL <http://stacks.iop.org/0022-3719/19/i=14/a=020>.
 - [3] R. H. Swendsen and J.-S. Wang, Phys. Rev. Lett. **57**, 2607 (1986), URL <https://link.aps.org/doi/10.1103/PhysRevLett.57.2607>.
 - [4] M. Doxastakis, Y.-L. Chen, O. Guzmán, and J. J. de Pablo, The Journal of Chemical Physics **120**, 9335 (2004), <https://doi.org/10.1063/1.1704634>, URL <https://doi.org/10.1063/1.1704634>.
 - [5] W. Im and C. L. Brooks, Journal of Molecular Biology **337**, 513 (2004), ISSN 0022-2836, URL <http://www.sciencedirect.com/science/article/pii/S0022283604001202>.
 - [6] H. G. Katzgraber, M. Palassini, and A. P. Young, Phys. Rev. B **63**, 184422 (2001), URL <https://link.aps.org/doi/10.1103/PhysRevB.63.184422>.